Spectro-spatial hyperspectral image reconstruction from interferometric acquisitions

Daniele Picone, Mohamad Jouni, Mauro Dalla Mura

{*daniele.picone, mohamad.jouni, mauro.dalla-mura*}*@grenoble-inp.fr*

I. Interferometric imaging systems

Multi-aperture Fabry-Perot interferometers [1-2]

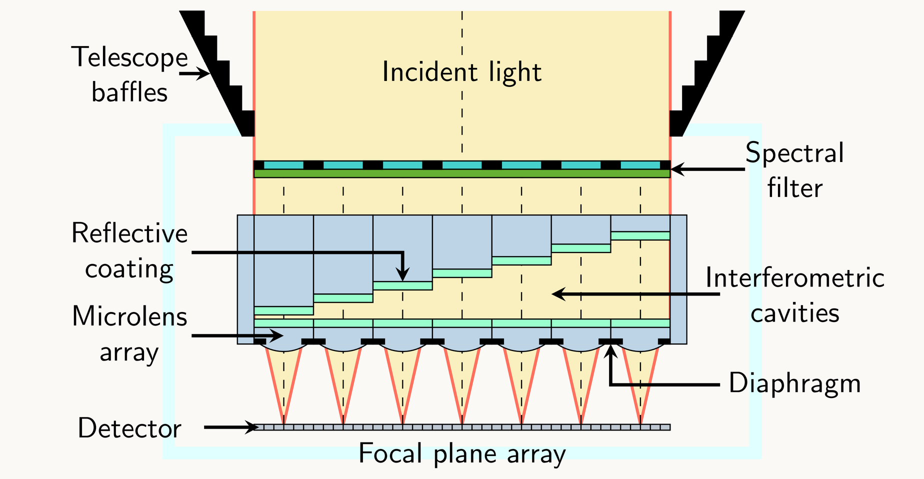

Optical design.

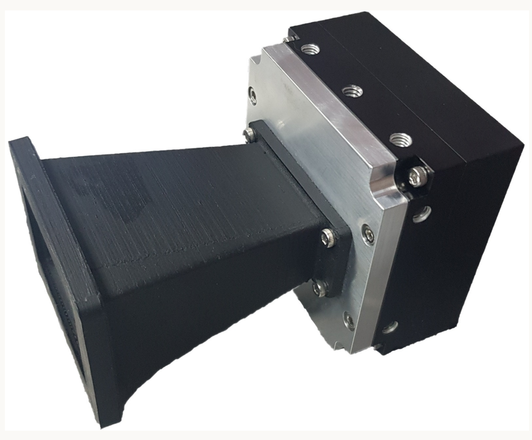

Device.

Scanning Fabry-Perot interferometers [3]

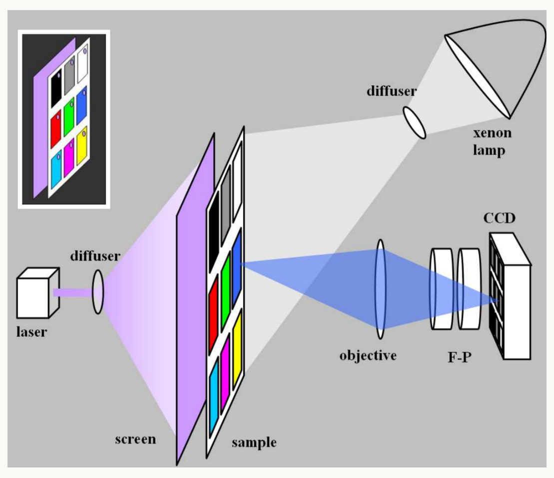

Optical design.

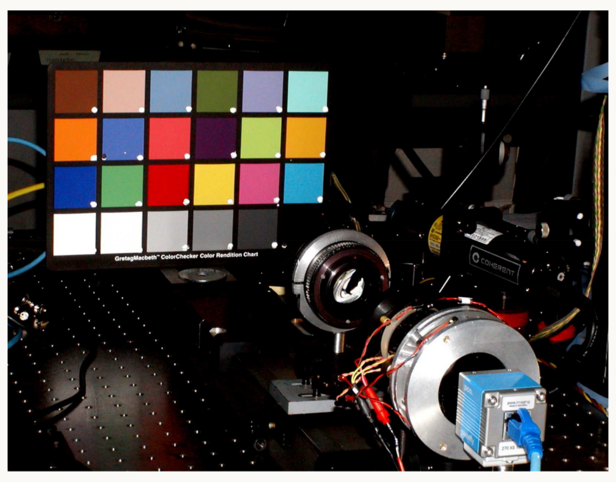

Device.

Birifrangent interferometers [4]

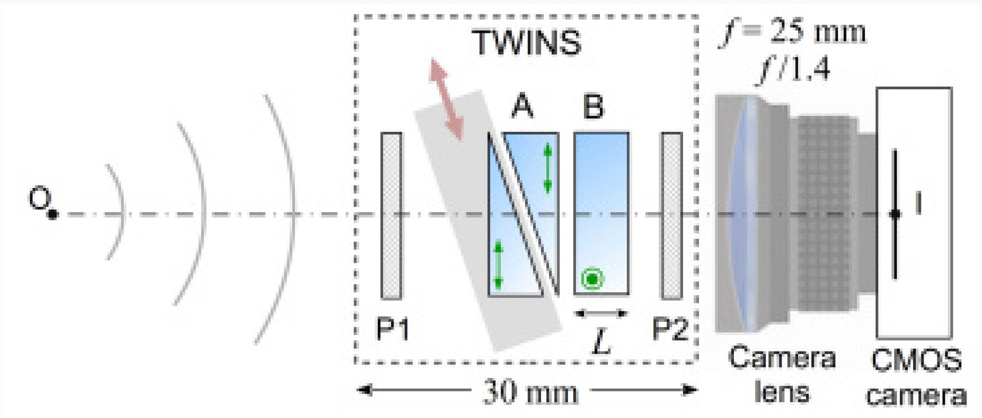

Optical design.

Device.

II. Spectrometers example acquisitions

Single pixel inteferometric spectrometer

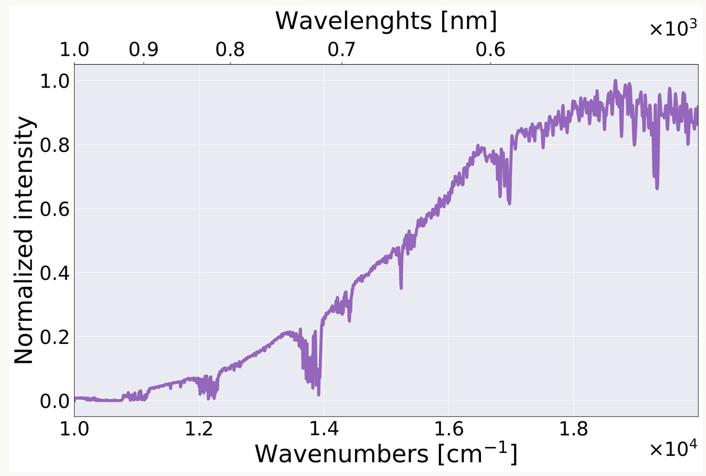

Wavelength domain.

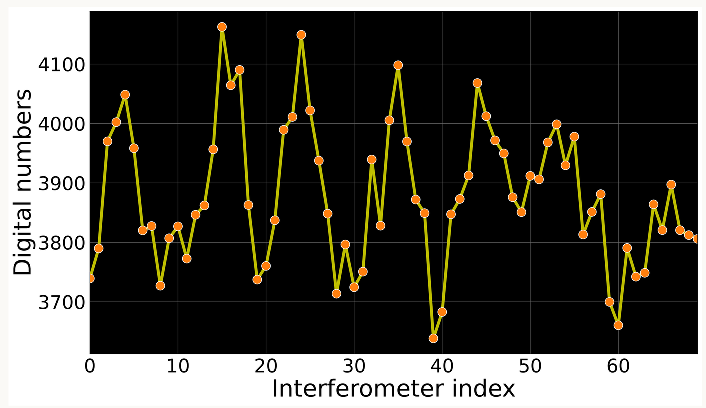

OPD domain.

Inteferometric imaging spectrometer [5]

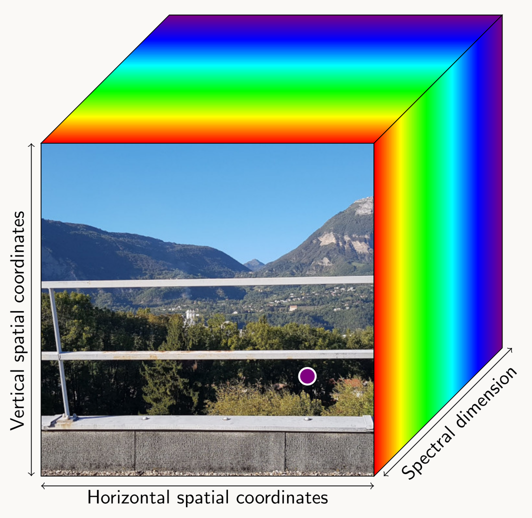

Image datacube $\mathcal{X} \in \mathbb{R}^{I \times J \times K}$.

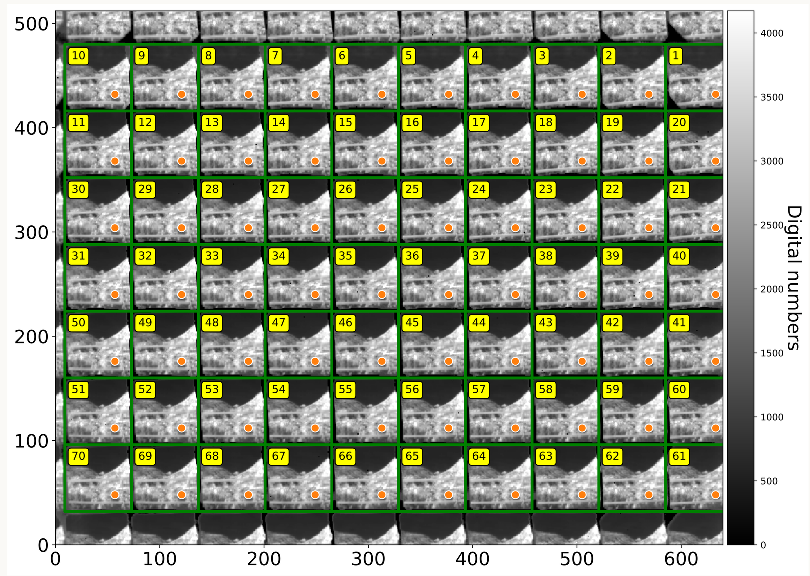

Acquisition $\mathcal{Y} \in \mathbb{R}^{I \times J \times L}$.

III. Problem statement

Objective: Estimate $\hat{\mathcal{X}}$: $\hat{\mathcal{X}} = \arg\min_{\mathcal{X}} \left(\frac{1}{2} \|\mathcal{X} \bullet_3 \mathbf{A} - \mathcal{Y}\|_2^2 + h(\mathbb{L}\mathcal{X}) \right)$.

- $f(\mathcal{X}) = \frac{1}{2} \|\mathcal{X} \bullet_3 \mathbf{A} - \mathcal{Y}\|_2^2$: data fidelity term.
- $g(\mathcal{X}) = h(\mathbb{L}\mathcal{X})$: prior (with linear operator $\mathbb{L}$).
- $\mathbf{A} \in \mathbb{R}^{K \times L}$: device transmittance function.

IV. Image reconstruction methodology

ADMM

$$\mathcal{Z}^{[q+1]} = \mathrm{prox}_{\tau f}\left(\mathcal{X}^{[q]} - \mathcal{U}^{[q]}\right)$$
$$\mathcal{X}^{[q+1]} = \mathrm{prox}_{\tau g}\left(\mathcal{Z}^{[q+1]} + \mathcal{U}^{[q]}\right)$$
$$\mathcal{U}^{[q+1]} = \mathcal{U}^{[q]} + \left(\mathcal{Z}^{[q+1]} - \mathcal{X}^{[q+1]}\right)$$

Loris-Verhoeven (LV)

$$\mathcal{Z}^{[q+1]} = \mathcal{X}^{[q]} - \tau\left(\nabla_f \mathcal{X}^{[q]} + \mathbb{L}^T \mathcal{U}^{[q]}\right)$$
$$\mathcal{U}^{[q+1]} = \mathrm{prox}_{\eta h^*}\left(\mathcal{U}^{[q]} + \eta \mathbb{L} \mathcal{Z}^{[q+1]}\right)$$
$$\mathcal{X}^{[q+1]} = \mathcal{X}^{[q]} - \tau\left(\nabla_f \mathcal{X}^{[q]} + \mathbb{L}^T \mathcal{U}^{[q+1]}\right)$$

- $\mathcal{X}^{[q]}$ is the estimation $\hat{\mathcal{X}}$ at the q-th iteration (with $\tau, \eta \in \mathbb{R}^+$).
- $\mathrm{prox}_{\gamma f}(\mathcal{X}) = \arg\min_{\mathcal{V}} \left(f(\mathcal{V}) + \frac{1}{2\gamma} \|\mathcal{V} - \mathcal{X}\|_2^2 \right)$ is the proximal operator of f.
- $h^*(\mathcal{X}) = \sup_{\mathcal{V}} (\langle \mathcal{V}, \mathcal{X} \rangle - h(\mathcal{V}))$ is the Fenchel conjugate of h

Approach 1: Spectro-spatial priors

$g(\cdot)$ operates in both domains:

- $\mathbb{L}(\mathcal{X})$: TV spatially, DCT spectrally.
- $h(\mathcal{X}) = \|.\|_{221}$ (ℓ_2 on gradients/bands, ℓ_1 on pixels).

Approach 2: Plug-and-Play [6]

- $\mathrm{prox}_{\tau g}$ is substituted with any denoiser, such as BM3D.
- $g(\cdot)$ is not necessarily known.

V. Reconstruction experiments

Setup

- Image to reconstruct:
  - 96 × 96 px.
  - 366 channels.
  - Wavelengths: [400, 700] nm.
- Simulated model $\mathbf{A} = \{a_{lk}\}$:

$$a_{lk} = \frac{(1 - \mathcal{R})^2}{1 + \mathcal{R}^2 - 2\mathcal{R} \sin^2(\frac{\pi \delta_l}{\lambda_k})} .$$

  - Reflectivity $\mathcal{R} = 0.255$.
  - OPD range: [0, 8000] nm.
  - OPD step size: 25 nm.
- SSIM values in parentheses.

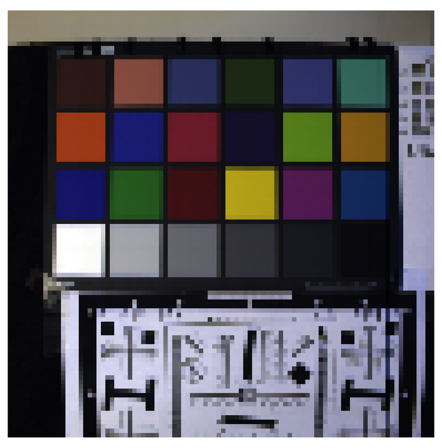

Reference (1.000)

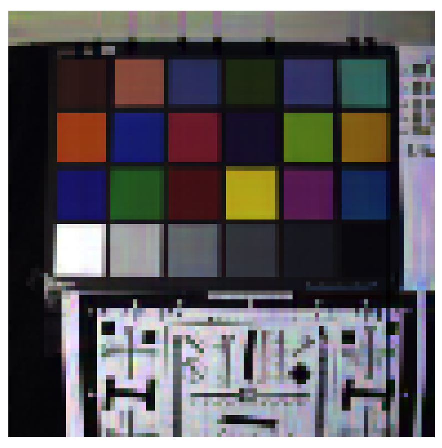

ADMM/BM3D (0.9853)

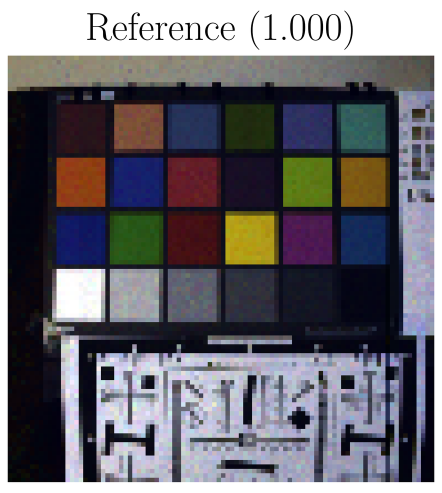

LV/DCT (0.9716)

LV/TV+DCT (0.9946)

VI. References

[1] Oiknine et al., "Multi-aperture snapshot compressive hyperspectral camera," Opt. Lett., vol. 43, no. 20, pp. 5042–5045, 2018.

[2] Gousset et al., "NanoCarb hyperspectral sensor: On performance optimization and analysis for greenhouse gas monitoring from a constellation of small satellites," CEAS Space Journal, vol. 11, no. 4, pp. 507–524, 2019.

[3] Pisani et al., "Compact imaging spectrometer combining Fourier transform spectroscopy with a Fabry-Perot interferometer," Opt. Express, vol. 17, no. 10, pp. 8319–8331, 2009.

[4] Perri et al., "Hyperspectral imaging with a TWINS birefringent interferometer," Opt. Express, vol. 27, no. 11, p. 15956, 2019.

[5] Picone et al., "Interferometer response characterization algorithm for multi-aperture Fabry-Perot imaging spectrometers," Opt. Express, vol. 31, no. 14, pp. 23066–23085, 2023.

[6] Venkatakrishnan et al., "Plug-and-Play priors for model based reconstruction," in IEEE GlobalSIP, 2013.

Grenoble Images Parole Signal Automatique

UMR CNRS 5216 - Grenoble Campus

38400 Saint Martin d'Hères - FRANCE